

Chapter 6. Atomic Force Microscopy

6.1 Introduction

The results from the thermal analysis study on the ethylene/ α -olefin copolymers presented in the previous chapter clearly indicate the existence of a dual crystallization mechanism in the copolymers. The results obtained were discussed in view of Flory's copolymer crystallization theory^{1,2}, and a working model for the crystallization mechanism in the copolymers was proposed, based on the ability of the (crystallizable) sequences to participate in the chain-folding lamellar growth process. It was suggested that the two different crystallization regions could be associated with two correspondingly different crystal morphologies. This suggestion is verified in the present study by a direct examination of the morphological features of the ethylene/ α -olefin copolymers by means of Atomic Force Microscopy (AFM). The technique (phase imaging) and the experimental details were discussed in Chapters 2 and 3, respectively. The micrographs obtained for the ethylene/1-butene copolymers of various comonomer contents are presented in this chapter. These micrographs provide concrete evidence for the morphological transformation discussed above and in the previous chapter.

It has been conclusively established from the results of the calorimetric studies presented in the previous chapter that the chemical nature of the branches (ethyl, propyl and butyl) does not influence the crystallization behavior, and consequently, the morphology of the copolymers. This conclusion is also sufficiently supported by similar results for such copolymers, available in the literature.^{3,4,5} It has been demonstrated by Minick *et al.*⁶ that the morphologies developed in statistical copolymers of ethylene/1-octene and ethylene/1-butene do not exhibit any observable difference with comonomer type. However, the specific details regarding the morphology of the secondary crystals were not clear in this study due to the staining technique employed to enhance contrast for TEM imaging.

6.2 Results

6.2.1 Effect of Comonomer Content on Morphology

The atomic force micrographs obtained at room temperature for the ethylene/1-butene copolymers of comonomer concentrations ranging from ~ 2 to 16 mole percent are shown in Figure 1 through Figure 6. The gradation in morphology with varying 1-butene concentrations is clearly seen by comparing these figures. In accordance with our expectation, the lowest-branched copolymer, EB-928, with only ~ 2 mole % 1-butene exhibits a highly ordered lamellar morphology, marked by long and thick lamellae (Figure 1). The predominant features in this micrograph are comparable to those observed for linear polyethylene.

The lamellar morphology still persists when the comonomer concentration is increased to ~ 5 mole % in EB-912 (Figure 2). However, both the thickness and the lateral dimensions of the lamellae are significantly reduced compared to those obtained from the micrograph of Figure 1 for EB-928. On increasing the 1-butene content to ~ 9 mole % in EB-894, further reduction in the dimensions of the lamellae occurs, resulting in their appearance as thin and short thread-like features (Figure 3). These reduced features preclude a meaningful evaluation of the lamellar thickness from the micrograph. The decreasing trend in the lamellar dimensions continues with increasing comonomer concentrations. For copolymers with greater than 9 mole percent 1-butene, the lateral dimensions of the lamellae are reduced so much that they are less clearly visible in the micrographs, which appear to exhibit a predominantly spot-like morphology (Figure 4, Figure 5 and Figure 6).

Identical results were obtained for the ethylene/1-pentene as well as ethylene/1-hexene copolymers. One example from each series is shown in Figure 7 and Figure 8 respectively. The samples indicated are the lowest branched copolymers of each series, namely EP-910 and EH-910 respectively. The lamellar morphology discerned in the micrograph of the corresponding ethylene/1-butene copolymer, EB-912 is also exhibited by these samples.

It is important to note that the samples with the highest comonomer contents are extremely tacky and present significant difficulties when examined in the tapping mode of the AFM. The main reason is the fact that the tapping head tends to get embedded in the soft and sticky sample, resulting in a micrograph overridden with lines and bright spots. Several attempts were necessary to collect presentable micrographs for these samples. It is also recognized that this difficulty could lead to spot-like features in the micrographs of highly branched samples. However, in the present study, careful experiments using

1. several different samples of a given copolymer
2. different tapping heads for a given sample, and
3. different magnifications of the observed features from a given sample

were performed, to yield reproducible results.

6.2.2 Dual Morphology

The morphology of the copolymer, EB-912 containing ~ 5 mole percent 1-butene is shown in Figure 2. Further magnification of the features in this figure provides evidence for the co-existence of the lamellae with bridge-like structures between the lamellae, and normal to their surfaces. Such a magnified micrograph is displayed in Figure 9. Although the bridge-like links can be discerned from the micrograph shown in the figure, it is noted that these features can be observed with remarkably greater clarity only when the lamellae between which they occur, appear edge-on on the micrographs.

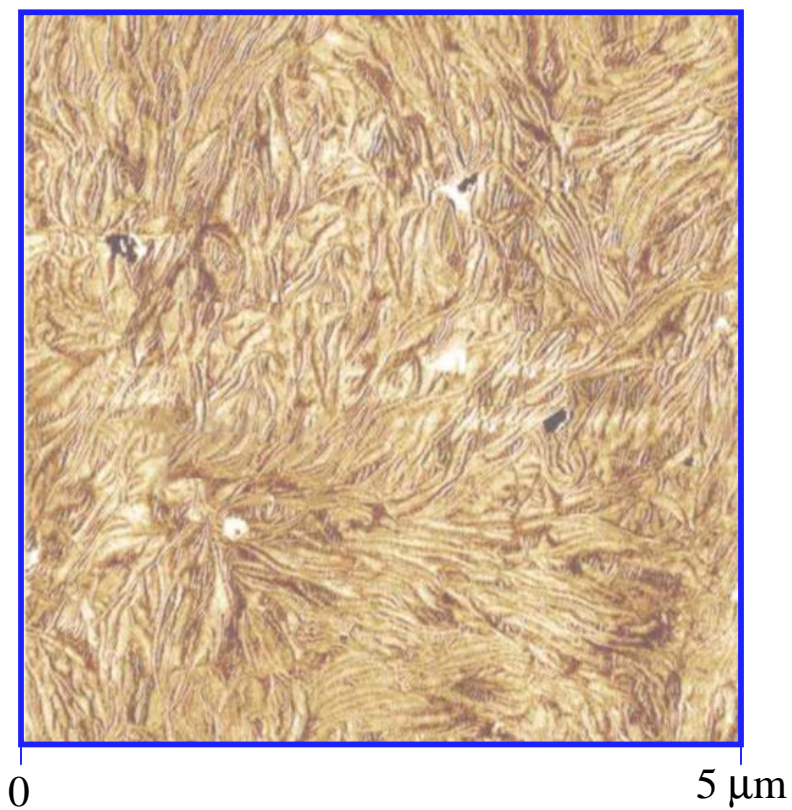


Figure 1 Atomic Force Micrograph of EB-928 (~2 mole % 1-butene);
Quenched sample (Cooling rate > 40°C/min)

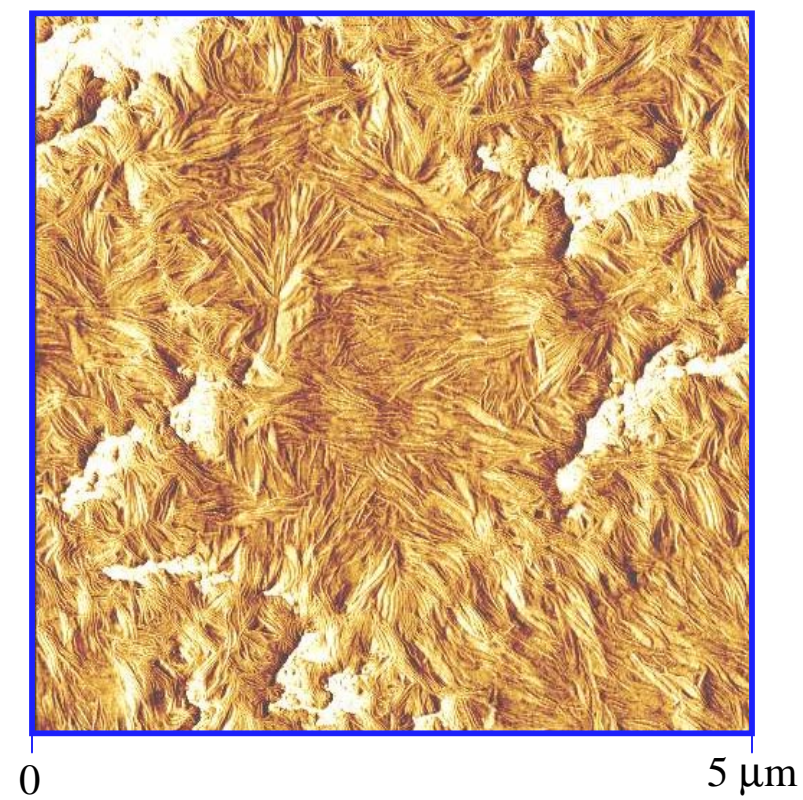


Figure 2 Atomic Force Micrograph of EB-912 (~5 mole % 1-butene);
Quenched sample (Cooling rate > 40°C/min)

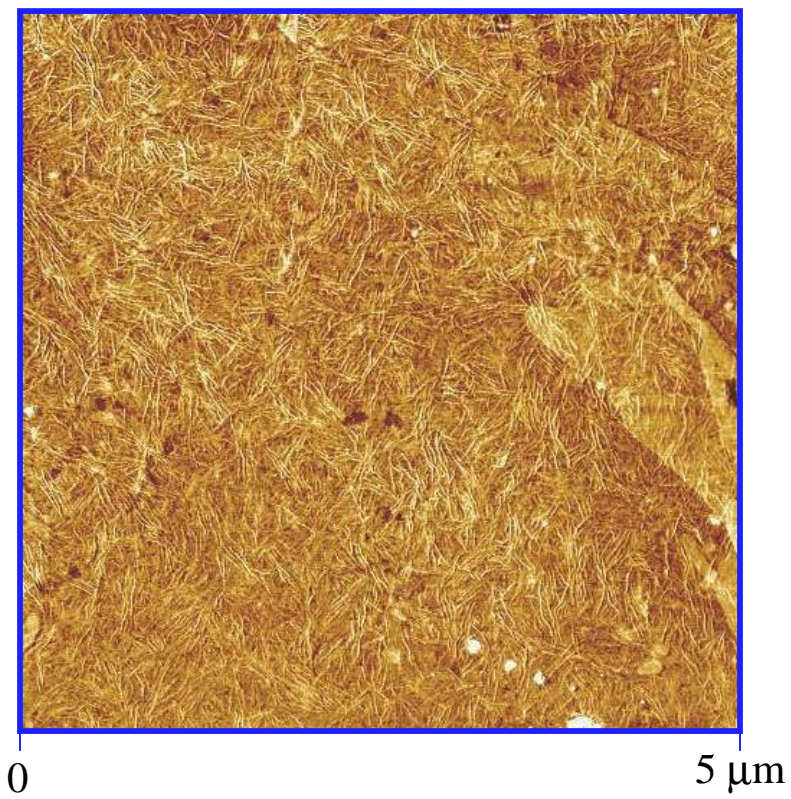


Figure 3 Atomic Force Micrograph of EB-894 (~9 mole % 1-butene);
Quenched sample (Cooling rate > 40°C/min)

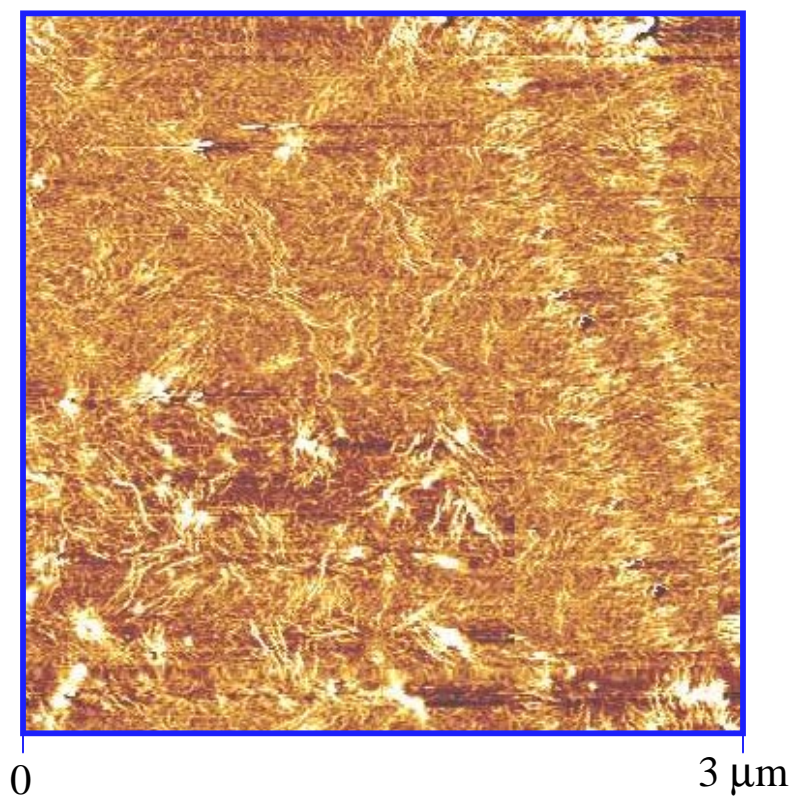


Figure 4 Atomic Force Micrograph of EB-883 (~13 mole % 1-butene);
Quenched sample (Cooling rate > 40°C/min)

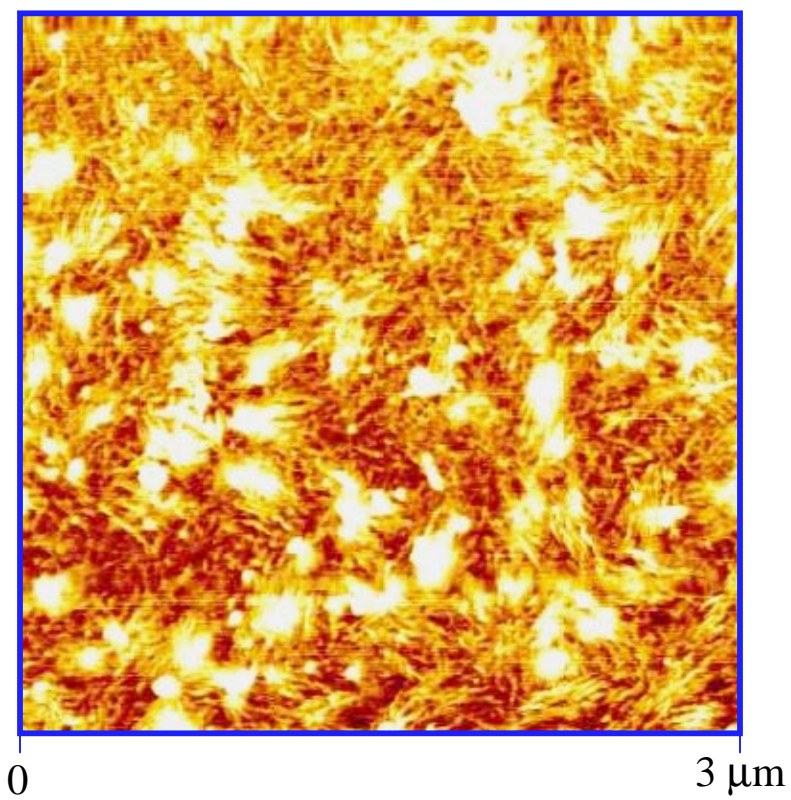


Figure 5 Atomic Force Micrograph of EB-879 (~14 mole % 1-butene);
Quenched sample (Cooling rate > 40°C/min)

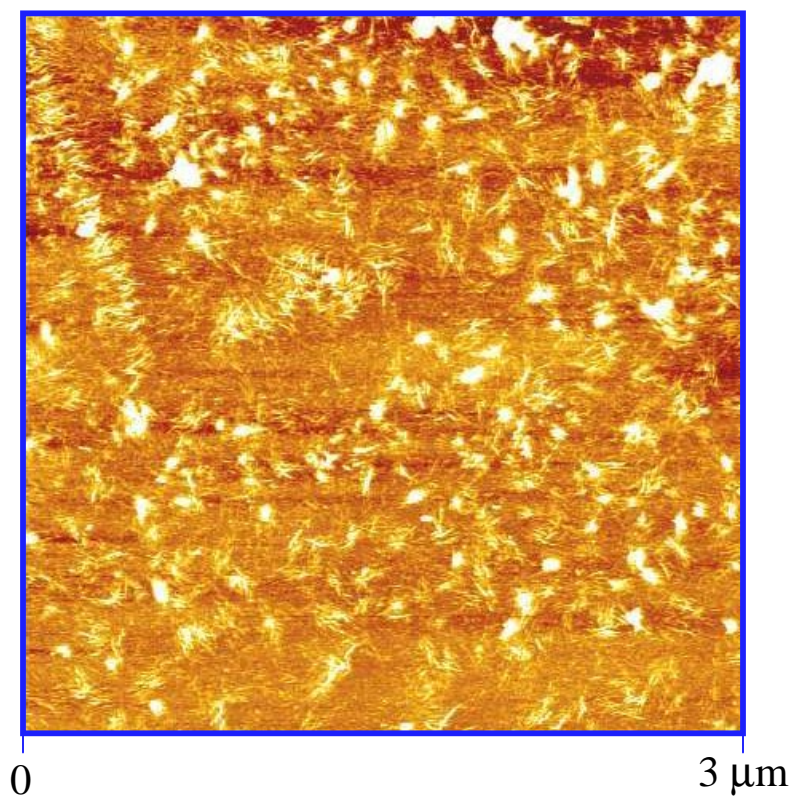


Figure 6 Atomic Force Micrograph of EB-874 (~16 mole % 1-butene);
Quenched sample (Cooling rate > 40°C/min)

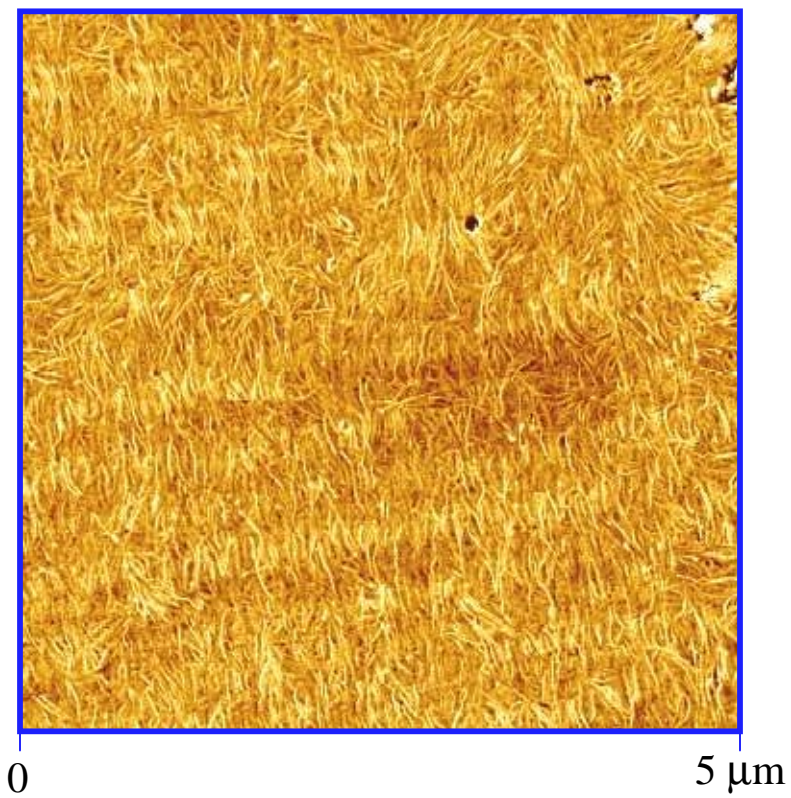


Figure 7 Atomic Force Micrograph of EP-910 (~ 5 mole % 1-pentene);
Quenched sample (Cooling rate > 40°C/min)

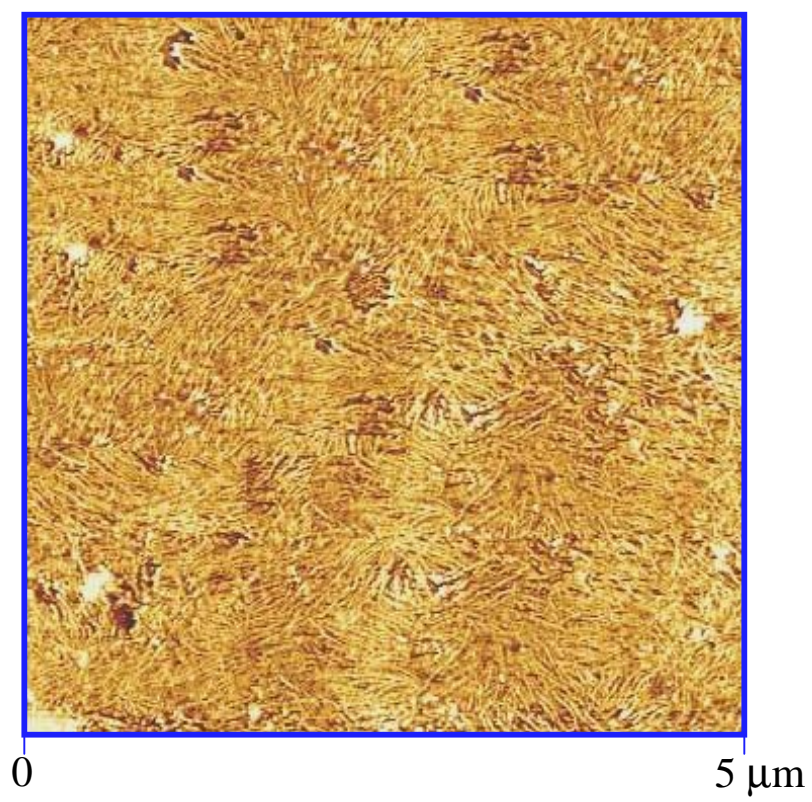


Figure 8 Atomic Force Micrograph of EH-910 (~ 4 mole % 1-hexene);
Quenched sample (Cooling rate > 40°C/min)

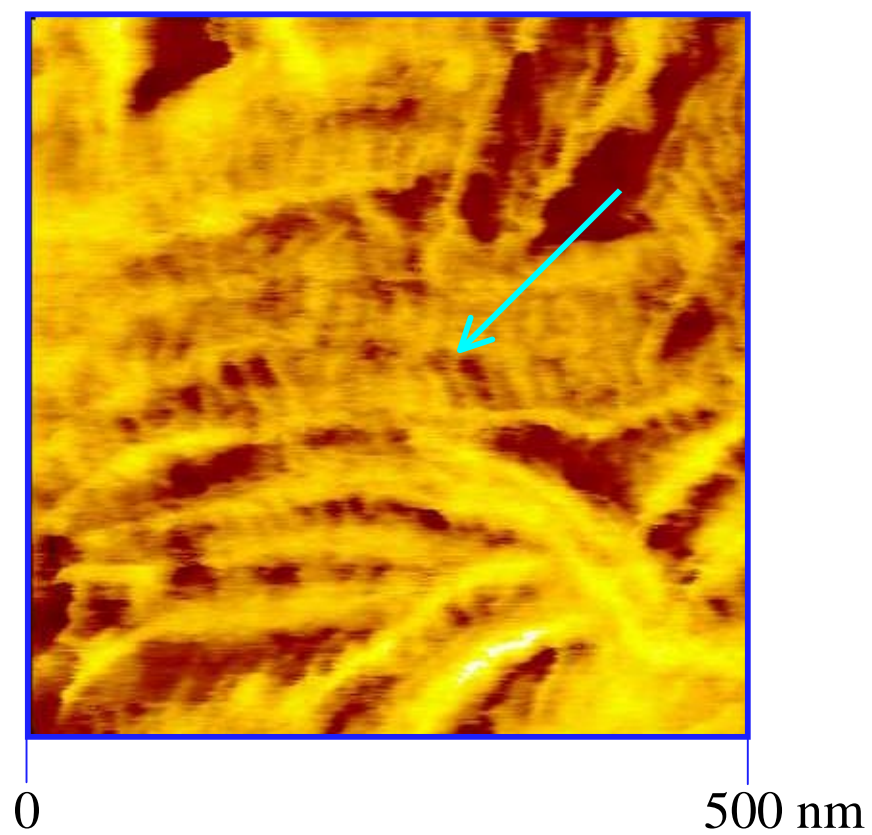


Figure 9 Atomic Force Micrograph of EB-912 (~5 mole % 1-butene) at a higher magnification; Quenched sample (Cooling rate > 40°C/min)

6.3 Discussion

6.3.1 Proposed Correlation between Comonomer Content and Morphology

When a copolymer is cooled from its melt, the longest sequences crystallize via chain-folding, resulting in the formation of lamellar crystals (primary crystallization). This process, however, pins down the remaining portions of the longest sequences as well as other shorter sequences at the lamellar crystal surface, thereby imposing tremendous constraints on the crystallizable sequences present in the inter-lamellar amorphous regions. At very high degrees of constraints, these sequences are unable to participate in the chain-folding process; however, they crystallize by simply aggregating into clusters with neighboring sequences^{7,8} to form "fringed-micellar" type bundled crystals (secondary crystallization). The lateral growth of these crystals is limited by the large stresses that develop at the crystal/melt interface in the absence of the chain-folding process.^{9,10} Therefore, the lateral dimensions of the bundled crystals are expected to be much lower than those of the lamellar crystals formed during the primary crystallization. This aspect is directly related to the reduced stability of the crystals, which causes them to melt at temperatures very close to their crystallization temperatures (discussed in the previous chapter).

It is clear from the above discussion that the distribution of crystallizable sequence lengths in a copolymer plays a significant role in the crystallization process. It is also known that the frequent occurrence of branches along the ethylene backbone fragments the copolymer chains into a number of segments, the longest of which can crystallize via chain folding. In a copolymer with a very low branch content, the number of such long segments capable of forming chain-folded lamellar crystals is large. The resulting crystals formed at the lowest undercoolings are characterized by significant lateral dimensions and thickness. However, as the branch concentration increases, the number of long sequences that can participate in the chain-folding process decreases correspondingly. In addition, the lengths of the longest sequences are also reduced compared to a lower-branched material. A combination of these two factors results in a decrease in the lateral dimensions as well as in the thickness and perfection of the

lamellar crystals formed from those sequences that do crystallize by chain-folding. At even higher branch concentrations, the number of long sequences is superseded by the number of shorter sequences that are unable to form chain-folded structures. This situation favors an increase in the population of the bundled crystals formed from the shortest sequences. Thus, it is expected that there is a gradual change in the predominant morphology of the copolymers from chain-folded lamellar crystals to "fringed-micelles"-like bundled crystals, with increasing comonomer contents.

6.3.2 Influence of Branch Concentration on Morphology

The sharp features of the lamellar morphology observed in the micrographs of the lowest-branched copolymer, EB-928 are consistent with the correlations proposed above. This sample contains only ~ 2 mole percent 1-butene. As a result, it has the largest number of crystallizable sequences available for regular chain folding, among all the copolymers examined. These sequences result in the formation of relatively thick lamellae with considerable lateral dimensions.

On increasing the comonomer content to ~ 5 mole percent (EB-912), the number of ethylene sequences long enough to form chain-folded lamellae decreases. In addition, the resulting chain folded crystals do not possess very high degrees of regular chain folding. For these reasons, thinner and smaller lamellae are observed for this material. However, in this case, there is a considerable fraction of crystallizable sequences trapped in the amorphous regions between the lamellae. As alluded to in the previous section, these sequences are highly constrained and their mobility is limited to local segmental motions only. As a result, they are incapable of participating in the reeling-in process required for the folding of chains to form lamellae. Instead, they aggregate locally with neighboring segments to form bundled crystals, with the chain axes approximately perpendicular to the surface of the primary lamellae. Then, it is possible to draw a correlation between these crystals and the bridge-like structures that appear normal to the lamellae (and in between them) in the micrograph of this sample (Figure 9).

The morphological aspects described in this chapter are not unique to the ethylene/1-butene copolymers. Similar observations have been made regarding the morphology of ethylene/1-octene copolymers¹¹ and ethylene/styrene interpolymers¹² also investigated in our laboratory. Accordingly, identical trends in the morphological features are obtained for the other two types of copolymers used in the present study, namely ethylene/1-pentene and ethylene/1-hexene copolymers.

It may be recalled from the discussion in Chapter 3 that the existence of a dual morphology in similar ethylene/ α -olefin copolymers has been proposed by other investigators.^{6,13,14,15} The co-existence of lamellar and granular type morphologies has been indicated in some of the studies.^{6,13} It is interesting to compare the dimensions of those granular structures ($\sim 6 - 12 \text{ nm}^{13}$) with the dimensions of the inter-lamellar bridges (a few nm) observed in the micrographs of the present study. The fact that the two dimensions are of the same order of magnitude provides further support for the correlation suggested above, between the bridge-like features from the micrographs and the bundled crystals that represent the second type of morphology present in the copolymers.

With increasingly higher branch concentrations, the number of sequences that can chain fold to form lamellar crystals further decreases. However, the few long sequences (shorter than the longest sequences in lower-branched copolymers) that do form lamellae pin down the remaining sequences at the lamellar surface, resulting in the constrained state alluded to in the previous section. In these samples, a greater fraction of crystallizable sequences are trapped and constrained in the inter-lamellar amorphous regions. As a result, the proportion of crystals formed from the shorter sequences increases. The lamellae become barely visible in the micrographs (Figure 4, Figure 5 and Figure 6).

6.3.3 Influence of Cooling Rate

The thermal analysis experiments reported indicate the existence of two regions of crystallinity variation with the cooling rate employed - a high temperature cooling rate

dependent region and a low temperature cooling rate independent region. The temperature range over which the cooling rate dependence is observed systematically decreases with increasing comonomer concentrations, until at the highest branch content, barely any cooling rate dependence is discerned. In agreement with these results, the AFM study of the highly branched copolymers indicates that their morphologies are invariant with the cooling rate, within the limits of resolution of the technique. This behavior of the highly branched copolymers may be contrasted to that of the lower branched copolymers that seem to display a considerable dependence on the cooling rate employed. The micrographs obtained for quenched and slowly cooled samples of EB-912, with ~5 mole percent 1-butene are shown in Figure 10. An observable difference in the length and thickness of the lamellae in the two micrographs is noted, and is consistent with the cooling rate dependence of the high temperature (chain-folded lamellae) region of the crystallinity vs. temperature curves mentioned above. Similar observations on the effect of thermal history (quenching and slowly cooling) on the morphology of ethylene/1-octene, ethylene/1-butene and ethylene/propylene copolymers have been made previously⁶ by means of TEM. The slowly cooled samples, unlike the quenched ones, displayed some long and curved lamellae that were ~ 140 Å thick with a few beaded strings and granules interspersed in the spaces in between. The edges between the lamellae and the adjacent stained regions were found to be well defined, indicating better surface order and a "possibility of chain folding".⁶ Similar variations of the lamellar features with varying crystallization conditions have also been reported for linear low-density polyethylenes.¹⁶

So far, the results from the AFM study on the ethylene/ α -olefin copolymers were discussed. It is suggested that the two crystallization regions associated with the DSC crystallinity curves may be related to the two different crystal morphologies, namely the chain-folded lamellae and the inter-lamellar bridge-like structures that are associated with the bundled crystals. In the next chapter, an investigation of the crystal structure associated with these two morphological forms is presented, by means of infrared spectroscopy experiments.

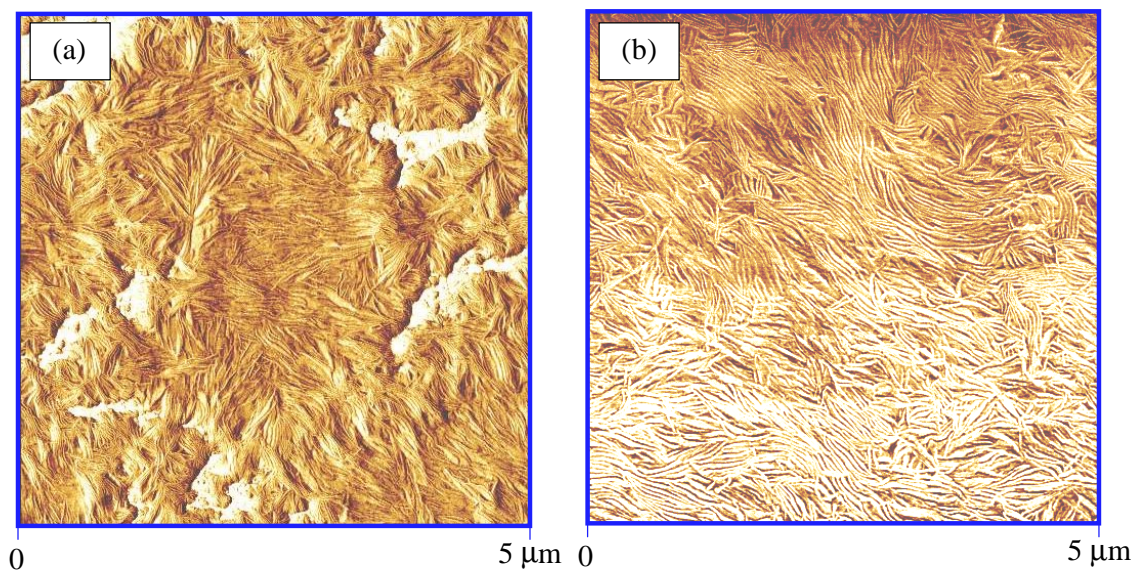


Figure 10 Atomic Force Micrograph of EB-912 (~5 mole % 1-butene) (a) quenched sample (cooling rate $> 40^{\circ}\text{C}/\text{min.}$) (b) slowly cooled sample (cooling rate = $1^{\circ}\text{C}/\text{min.}$)

-
- ¹ P. J. Flory, *J. Chem. Phys.*, **17**, 3, 223 (1949)
 - ² P. J. Flory, *Trans. Faraday Soc.*, **51**, 848 (1955)
 - ³ R. Alamo, R. Domszy and L. Mandelkern, *J. Phys. Chem.*, **88**, 6587 (1984)
 - ⁴ R. G. Alamo and L. Mandelkern, *Macromolecules*, **22**, 1273 (1989)
 - ⁵ R. G. Alamo and L. Mandelkern, *Thermochim. Acta*, **238**, 155 (1994)
 - ⁶ J. Minick, A. Moet, A. Hiltner, E. Baer and S. P. Chum, *J. Appl. Polym. Sci.*, **58**, 1371 (1995)
 - ⁷ P. J. Flory and A. D. McIntyre, *J. Polym. Sci.*, **18**, 592 (1955)
 - ⁸ M. Takayanagi and T. Yamashita, *J. Polym. Sci.*, **22**, 552 (1956)
 - ⁹ C. M. Guttman, E. DiMarzio and J. D. Hoffman, *Polymer*, **22**, 1466 (1981)
 - ¹⁰ J. D. Hoffman and R. L. Miller, *Polymer*, **38**, 3151 (1997)
 - ¹¹ A. Alizadeh, L. Richardson, J. Xu, S. McCartney and H. Marand, *Submitted to Macromolecules*
 - ¹² A. Alizadeh, J. Xu, T. J. Moreland, S. Christian, E. Marand and H. Marand, *Bull. Am. Phys. Soc.*, (1999)
 - ¹³ V. B. F. Mathot, R. L. Scherrenberg and T. F. J. Pijpers, *Polymer*, **39**, 4541 (1998)
 - ¹⁴ R. A. C. Deblieck and V. B. F. Mathot, *J. Mater. Sci. Let.*, **7**, 1276 (1988)
 - ¹⁵ F. M. Mirabella Jr., S. P. Westphal, P. L. Fernando, E. A. Ford and J. G. Williams, *J. Polym. Sci. Polym. Phys.*, **26**, 1995 (1988)
 - ¹⁶ I. G. Voigt-Martin, R. Alamo and L. Mandelkern, *J. Polym. Sci. Polym. Phys.*, **24**, 1283 (1986)